Anesthesiology 2003; 99:112–21

Improved Resuscitation after Cardiac Arrest in Rats Expressing the Baculovirus Caspase Inhibitor Protein p35 in Central Neurons

Peter Vogel, Ph.D., Herman v.d. Putten, Ph.D.,† Erik Popp, M.D.,* Jakub J. Krumnikl, M.D.,* Peter Teschendorf, M.D.,* Roland Galmbacher, B.S.,‡ Malgorzata Kisielow, B.Sc.,§ Christoph Wiessner, Ph.D.,† Albert Schmitz, Ph.D.,† Kevin J. Tomaselli, Ph.D.,‖ Bernd Schmitz, M.D.,# Eike Martin, M.D.,** Bernd W. Böttiger, M.D.††*

Background: **Global cerebral ischemia is associated with delayed neuronal death. Given the role of caspases in apoptosis, caspase inhibitors may provide neuronal protection after cardiac arrest. To this end, the authors generated a transgenic rat line expressing baculovirus p35, a broad-spectrum caspase inhibitor, in central neurons. Its effects were evaluated on neuronal cell death and outcome after global cerebral ischemia.**

Methods: **Global cerebral ischemia was induced by cardiocirculatory arrest. After 6 min, animals were resuscitated by controlled ventilation, extrathoracic cardiac massage, epinephrine, and electrical countershocks. Neuronal death was assessed after 7 days by histologic evaluation of the hippocampal cornu ammonis 1 sector. Postischemic outcome was assessed by determination of overall survival and according to neurologic deficit scores 24 h, 3 days, and 7 days after resuscitation.**

Results: **The rate of 7-day survival after cardiac arrest for the transgenic rats (85%) was significantly higher than that for the nontransgenic controls (52%; $P < 0.05$). However, no differences were observed either in the number of terminal deoxynucleotidyltransferase–mediated d-uracil triphosphate–biotin nick end-labeling–positive cells or viable neurons in the cornu ammonis 1 sector or in the neurologic deficit score when comparing surviving transgenic and nontransgenic rats. These findings suggest that neuronal apoptosis after cardiac arrest is not primarily initiated by activation of caspases.**

Conclusion: **Expression of baculovirus p35 can improve survival after cardiac arrest in rats, but the mode and site of action remain to be elucidated.**

CARDIAC arrest is the most important cause of global cerebral ischemia, with only 2–12% of resuscitated patients being discharged from the hospital without neurologic dysfunction. Clinical attempts to improve neurologic outcome after cardiac arrest by focusing on brain protection *via* the use of barbiturates and on reperfusion injury with the use of calcium channel blockers have failed.[1,2] The only specific treatment option to improve clinical neurologic outcome is mild hypothermia in selected patients.[3–7]

More recent experimental efforts have focused on selective neuronal vulnerability and microcirculatory reperfusion disorders.[8,9] Even brief periods of cerebral ischemia result in delayed neuronal death in vulnerable areas of the brain, such as the cornu ammonis 1 (CA-1) sector of hippocampus and the thalamic reticular nucleus.[10,11] Neuronal apoptosis plays an important pathophysiologic role in this process. Current concepts of apoptosis suggest that caspases, the cysteine aspartyl-specific proteases,[12–14] are involved in the final steps of cell death cascades. After transient global cerebral ischemia in rats, an increase in caspase 3 messenger RNA (mRNA) expression in vulnerable hippocampal CA-1 neurons and a concomitant increase in caspase 3–like proteolytic activity in hippocampal protein extracts could be detected.[15] Further evidence for a role of caspases in neuronal damage after cerebral ischemia in rodents is seen in the reductions in infarct volume obtained after permanent focal ischemia by pharmacologic inhibitors of caspases,[16–18] by transgenic overexpression of a dominant negative caspase 1 mutant,[19] and by ablation of the caspase 1[20] and caspase 11 gene.[21] Furthermore, oligodendrocytes derived from transgenic mice overexpressing the broad-spectrum baculovirus caspase inhibitor p35 are protected against *in vitro* hypoxia and *in vivo* focal ischemia, as measured by caspase 3 activation.[22] Thus, inhibition of caspases and/or apoptosis could provide neuroprotective strategies in cerebral ischemia and neurodegenerative disease.[23]

In vitro and *in vivo* inhibition of caspases has been achieved by synthetic caspase inhibitor compounds and by viral proteins that act as natural caspase inhibitors. The latter include the cowpox virus protein CrmA and the baculovirus protein p35.[24,25] p35 is an active, site-specific inhibitor of caspases, with a high capacity to inhibit caspase 3.[24] p35 is cleaved at the following amino acid sequence: aspartic acid–glutamine–methionine–aspartic acid–glycine. The cleaved products (25 and 10 kD) dissociate from the caspase slowly, if at all.[13] *In*

This article is featured in "This Month in Anesthesiology." Please see this issue of ANESTHESIOLOGY, page 5A.

* Research Fellow, ‡ Technical Assistant, ** Professor, Head of the Department of Anesthesiology, †† Assistant Professor, Department of Anesthesiology, University of Heidelberg. † Senior Scientist, Nervous System Research, Novartis Pharma AG, Basel, Switzerland. ‖ Senior Scientist, IDUN Pharmaceuticals, La Jolla, California. § Ph.D. Student, Institute for Biomedical Research, Bellinzona, Switzerland. # Assistant Professor, Department of Anesthesiology, University of Erlangen, Erlangen, Germany.

Received from the Department of Anesthesiology, University of Heidelberg, Heidelberg, Germany. Submitted for publication July 10, 2002. Accepted for publication March 12, 2003. Supported by grants from the Medical Faculty of the University of Heidelberg and by the Deutsche Forschungsgemeinschaft (Bo 1686/1-1), Bonn, Germany. Presented at a meeting of the Society of Neurosurgical Anesthesia and Critical Care Medicine for the Young Investigators Award, New Orleans, Louisiana, October 12, 2001.

Address reprint requests to Dr. Böttiger: Department of Anesthesiology, University of Heidelberg, Im Neuenheimer Feld 110, D-69120 Heidelberg, Germany. Address electronic mail to: bernd_boettiger@med.uni-heidelberg.de.

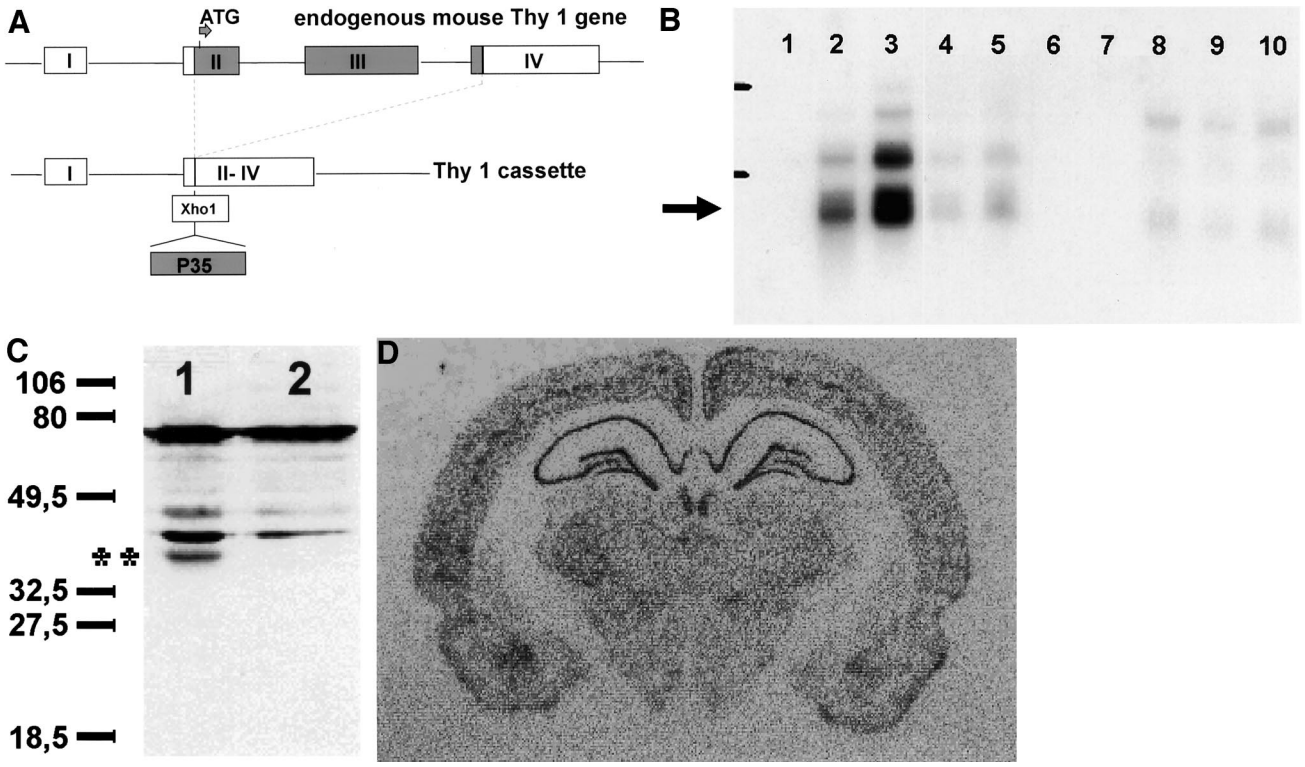

Fig. 1. Construction and expression of p35 in the rat brain. (*A*) Schematic drawing of the Thy1 expression cassette with insertion of p35 complementary DNA using an *Xho*I restriction site. (*B*) Northern blot analysis of Thy1EμP35 transgenic rats. *Lanes 1–3* contain 3 μg per lane polyA+ brain RNA from nontransgenic rats (*lane 1*), line L25 rats (*lane 2*), and line L24 rats (*lane 3*). *Arrow* indicates p35 messenger RNA. *Bars* show the ribosomal position of 28S and 18S RNA. *Lanes 4–10* contain 10 μg per lane total RNA from rat brain (*lanes 4–6*) and thymus (*lanes 7–10*) of transgenic animals (*lanes 4, 5, 8, 9,* and *10*) and nontransgenic littermates (*lanes 6* and *7*). (*C*) Western blot analysis of brain extracts from transgenic rats. *Lane 1* = transgenic rat line L24; *lane 2* = nontransgenic rat brain extract. *Asterisks* show position of p35 protein in gel. (*D*) *In situ* hybridization analysis of p35. The image of the transgenic Thy1EμP35 rat brain is shown at the hippocampal level; no background signal was detected in brains of the control group (data not shown).

vitro, p35 can also inhibit caspases 1, 2, 6, 7, 8, and 10.[13,24] p35 is a broad-spectrum inhibitor of death pathways that, in mammalian cells, has been shown to inhibit apoptosis induced by tumor necrosis factor or CD95 ligation or by glucocorticoids, ionizing radiation, DNA damaging agents, ceramides, and growth factor withdrawal.[24,26–31]

We, therefore, generated a transgenic rat line expressing the antiapoptotic baculovirus protein p35 (fig. 1) to determine whether there are beneficial effects on the outcome of rats resuscitated from global ischemia caused by cardiocirculatory arrest.

Materials and Methods

After institutional approval by the Governmental Animal Care Committee was obtained, 13 adult heterozygotic p35 transgenic rats (Wistar Thy1EμP35) and 25 nontransgenic littermates (body weight, 320–450 g) were obtained for a blinded, randomized trial. The transgenic animals and the nontransgenic control animals could not be distinguished from each other by color, size, weight, behavior, fertility, or any of the physiologic parameters measured (table 1). All animals were handled according to the Guiding Principles published by the National Institutes of Health and the Council of the American Physiologic Society (National Institutes of Health, 1985). The difference in the number of trans-

Table 1. Comparison of Relevant Physiologic and Blood Parameters between p35 and Nontransgenic Animals (Wild-type) during the Steady-state Phase preceding Cardiac Arrest

	p35	Wild-type
Body weight (g)	274.6 ± 92.3	289.6 ± 98.8
Mean arterial blood pressure (mmHg)	89.4 ± 14.9	87.1 ± 15.8
Temperature (°C)	37.3 ± 0.2	37.3 ± 0.2
pH	7.4 ± 0.1	7.4 ± 0.1
P_{CO_2} (mmHg)	38.9 ± 5.7	39.5 ± 6.3
P_{O_2} (mmHg)	150.7 ± 75.3	148.3 ± 38.0
HCO_3 concentration (mM)	22.6 ± 3.2	22.6 ± 1.9
Base excess (mM)	−2.4 ± 3.5	−2.7 ± 2.3
Hemoglobin concentration (g/dL)	11.8 ± 1.5	11.9 ± 1.1
Hematocrit (%)	34.5 ± 4.3	34.2 ± 5.9
K^+ concentration (mM)	3.3 ± 0.5	3.4 ± 0.5

Values are expressed as mean ± SD.

No statistically significant differences could be seen between the two groups.

genic animals and their nontransgenic littermates after deblinding was due to the breeding results.

Transgenes

The Thy1EμP35 transgene was constructed by inserting p35 into the unique *Xho*I site of the Thy1Eμ expression cassette (fig. 1, *A*) that yields brain, thymocyte, and peripheral T cell expression.[32,33] A p35 complementary DNA was inserted that was generated by polymerase chain reaction analysis using *Xho*I site–containing oligos (5'-GCTCGAGCATTGCAAAATGTGTGTA-3' and 5'-AGAGCTCTTATTTAATTGTGTTTAATATTAC-3') and the plasmid pSP35K as a template. pSP35K comprises a 1,118-base pair blunted *Nru*I–*Eco*RI p35-encoding DNA fragment excised from P35KORF and cloned into blunted *Hin*cII–*Eco*RI pSP64.

DNA Microinjection

A Thy1EμP35 plasmid- and vector-free DNA fragment was isolated using a standard procedure[32] and dissolved in 5 mM tris(hydroxymethyl)aminomethane–HCl (pH 7.6), 0.1 mM EDTA at a concentration of 2–4 μg/ml for DNA microinjection. Thy1EμP35 rats were generated on a Wistar background.

Genotyping

For Southern blot analysis, we used 10 μg of *Sac*I-digested DNA per gel lane. A 600-base pair *Xho*I–*Bam*HI fragment of Thy1, comprising part of exon 4, and a 1.1-kilobase *Xho*I fragment, comprising p35 complementary DNA, were used as probes. Probes were labeled with [α-^{32}P]-2'-deoxycytidine-5'-triphosphate using a random priming kit. Hybridizations were performed at 42°C in 50% formamide, 5× standard saline citrate, 2× Denhardt solution, 1% sodium dodecyl sulfate, 20 mM phosphate buffer, 10 mM EDTA, and 1 mg/ml denatured herring sperm DNA.

Polymerase chain reaction genotyping was done using either two internal p35 oligonucleotides (P35F1, 5'-TACGACGTCGTAGCTTACGT-3'; P35R1, 5'-CTAAAGCCTTGTAGATCATGC-3') or a Thy1Eμ expression cassette–specific oligonucleotide (5'-AGGAAGCAGGTCATGTGGCAAGG-3' in Eμ) in combination with a p35-specific oligo (P35R2, 5'-CGAATAATCGTCTGGGACACGTC-3').

Northern Blot Analysis

Total RNA was isolated from brain and/or thymus using TRIzol reagent according to the manufacturer's instructions (Gibco BRL Life Technologies GmbH, Karlsruhe, Germany). Of the denatured RNA, 10 μg was separated on 0.8% agarose formaldehyde gels, transferred onto a GeneScreen membrane (Genescreen, Dallas, TX) in 10× standard saline citrate, and fixed by baking for 2 h at 80°C. Probes were labeled with [α-^{32}P]-2'-deoxycytidine-5'-triphosphate using a random priming kit, and hybridizations were performed at 42°C in 50% formamide containing 5× standard sodium citrate, 2× Denhardt solution, 1% sodium dodecyl sulfate, 20 mM phosphate buffer, 10 mM EDTA, and 1 mg/ml denatured herring sperm. A 1.1-kilobase *Xho*I fragment spanning p35 was used as probe (see previous section) (fig. 1, *B, lanes 4–10*). Transgene expression was also analyzed using polyadenylated RNA Northern blots (fig. 1, *B, lanes 1–3*). The polyadenylated RNA was isolated from the total RNA using the Oligotex mRNA method. The amounts of polyadenylated RNA loaded per lane were 3 μg (brain) and 2 μg (thymus). The blots were probed with random-primed p35 probe.

In Situ *Hybridization*

The 1-kilobase p35 probe used for *in situ* hybridization was subcloned in pLitmus28 (antisense was made using T7 polymerase after linearization with *Spe*I; sense probes were generated using T7 polymerase after linearization with *Afl*II). Probes were labeled with uridine-5'-[α-^{35}S]-triphosphate and adenosine-5'-[γ-^{35}S]-thiotriphosphate as described previously.[34]

Western Blot Analysis

To monitor p35 expression, hippocampal preparations were incubated on ice in 1 ml ice-cold extraction buffer (20 mM HEPES–KOH [pH 7.5], 10 mM KCl, 1.5 mM $MgCl_2$, 1 mM EDTA, 1 mM dithiothreitol, 0.1 mM phenylmethylsulfonyl fluoride, 250 mM sucrose, and 1 mM *N*-benzoylcarbonyl–valine–alanine–aspartic acid–fluoromethylketone (zVADfmk) containing protease inhibitors [Complete TM Tablets; Roche Diagnostics, Mannheim, Germany]). After centrifugation (1,000*g*), the supernatant was centrifuged again (14,000*g* for 30 min at 4°C). The pellet was resuspended in 250 μl buffer, and 20-μl extracts were run per lane on 12% sodium dodecyl sulfate–polyacrylamide gel electrophoresis. After electroblotting, membranes were incubated overnight with polyclonal antibodies to p35 (1:1,000; kindly provided by IDUN Pharmaceuticals, San Diego, CA), followed by a 1-h incubation with alkaline phosphatase–conjugated antibody to rabbit immunoglobulins (1:5,000; Jackson ImmunoResearch, West Grove, PA). A Chemiluminescent Detection System (Clontech, Heidelberg, Germany) was used to detect p35. For comparing expression levels of p35 across different types of tissues, total protein levels were measured (Micro BCA Protein Assay Kit; Pierce, Rockford, IL), and equal amounts of protein were loaded on sodium dodecyl sulfate–polyacrylamide gel electrophoresis.

Animal Preparation

After induction of anesthesia with halothane (0.8–2.0%) and 70% N_2O in O_2, the animals were endotracheally intubated (Braunüle-MT No. 3; B. Braun, Melsungen, Germany) and mechanically ventilated (Harvard Rodent Ventilator; Harvard Apparatus, South Natick, MA). Poly-

ethylene catheters (PE 50) were inserted into the left femoral artery and vein. Heparin was not given during the entire study period. The tidal volume was adjusted to ensure a $Paco_2$ within the physiologic range as analyzed by arterial blood gas analysis. The fraction of inspired oxygen concentration was adjusted to maintain a Pao_2 of greater than 100 mmHg. The arterial catheter line was connected to a pressure transducer (Kombidyn Monitoring Set; B. Braun), which was leveled to mid-heart. The transducer output was displayed and recorded continuously (DASYLab Software; Datalog, Mönchengladbach, Germany).

Electrocardiographic recordings were performed using subcutaneous needle electrodes. All animals received an esophageal electrode for transesophageal induction of electrical ventricular fibrillation. The tympanal temperature of the animals was maintained within a range of 37°–37.4°C by a heating fan as long as the trachea was intubated before and after cardiac arrest.

Experimental Protocol

Three minutes before cardiac arrest, N_2O, but not halothane, was discontinued. Cardiac arrest was induced by electrical stimulation (alternating current: 12 V, 50 Hz) *via* the esophageal electrode[35] and confirmed by the abrupt decrease in mean arterial pressure to less than 15 mmHg. Ventilation was stopped, and the heating system was switched off. After 6 min of cardiac arrest, cardiopulmonary resuscitation procedures were begun, including mechanical ventilation (100% O_2; respiratory rate, 45 per minute; initiated 15 s before cardiac massage), closed chest cardiac massage (200 times per minute), and intravenous bolus administration of 0.02 mg/kg epinephrine and 0.5 mEq/kg $NaHCO_3$. If necessary, after 2 min, external defibrillation (5 Ws) (DC-defibrillator DEFIPORT SCP912; Hellige, Freiburg, Germany) was carried out. If restoration of spontaneous circulation (ROSC) was not achieved immediately, direct current countershocks were repeated after 30–60 s and accompanied by continuation of cardiopulmonary resuscitation procedures. ROSC was confirmed by spontaneous cardiac rhythm in conjunction with a rise in mean arterial pressure to greater than 50 mmHg. The heating fan was switched on immediately after ROSC, and the saline infusion was resumed. Blood gas analyses were performed 5 min and 20 min after ROSC, and the ventilatory parameters were adjusted, if necessary. If the base excess exceeded −5 mEq, additional $NaHCO_3$ was administered. If ROSC could not be achieved within 6 min, the resuscitation procedures were stopped.

The animals were weaned from the ventilator after stepwise reduction of the fraction of inspired oxygen concentration to 0.4 and allowed to breathe spontaneously at 1 h after ROSC. Catheters were removed, and the wounds were infiltrated with lidocaine, 1% (Xylocain; Astra, Wedel, Germany), and properly closed. Afterward, they were placed in special cages with O_2 concentrations of about 50% for several hours. Thereafter, animals were returned to their home cages with free access to food and water. They received 20 ml per day lactated Ringer's solution subcutaneously until they started drinking.

An investigator who was blinded to the experimental animal groups performed resuscitation. After the animals had survived for 7 days, they were killed, and then the brains were removed and postfixed overnight in paraformaldehyde before embedding and sectioning. At the hippocampal level (approximately at bregma, −3.5 mm), 5-μm coronal sections of brain were cut and placed on polylysine-coated glass slides.

Neurologic Deficit Score

To evaluate the neurologic state in all successfully resuscitated animals, the neurologic deficit score (NDS) was determined at 1, 3, and 7 days after cardiac arrest. The NDS was determined according to Katz *et al.*[36] and Neumar *et al.*[37] Scoring includes five parameters: general behavior, cranial nerve function, motor function, sensory function, and coordination. An NDS of 0% reflects normal brain function, and an NDS of 100% reflects brain death. The neurologic recovery was defined as the difference between NDSs after day 1 and day 7. If the neurologic recovery was greater than 30 points, this was defined in advance as an improved neurologic recovery. In contrast, if the difference in the neurologic scores was lower than 30, we defined this as a worse capability for recovery. The same investigator, who was blinded to the experimental animal groups, always performed the evaluation.

Morphology

For *in situ* staining of DNA fragmentation and apoptotic bodies, the histochemical terminal deoxynucleotidyltransferase–mediated d-uracil triphosphate–biotin nick end-labeling (TUNEL) method[38] was used as described previously.[39] The CA-1 sector of the hippocampus was analyzed by counting TUNEL-positive cells in the visual field of the microscope (magnification, 400-fold). TUNEL staining was used to determine the extent of neurodegeneration in the examined CA-1 sector of the hippocampal area. In addition, on the basis of the morphologic characteristics, the type of cell death was classified as apoptotic or necrotic. Criteria for an apoptotic-like cell death were intense staining of condensed chromatin (in contrast to diffuse staining of the complete nucleus) and the presence of apoptotic bodies, small or mid-sized extubations of the nucleus filled with condensed chromatin stained dark brown, which both could be detected in cells with an apparently normal cell shape (preservation of the cellular membrane).

Histologic examination was performed on Nissl-stained 5-μm sections at the level of the dorsal hippocampus. The neuronal degeneration of the CA-1 sec-

tor of the hippocampus was analyzed as described above by counting the viable neurons in the visual field by the same investigator, who was blinded to the experimental animal groups.

Statistical Analysis

For intergroup comparison, physiologic and hemodynamic variables, TUNEL staining, and viability of neurons were analyzed on a pairwise basis (*t* test). Statistical analysis of the NDS was performed using multifactorial ANOVA for repeated measurements followed by *t* test with Bonferroni correction. Neurologic recovery (day 1 NDS − day 7 NDS) and survival were analyzed by the chi-square test and Fisher exact test using the fourfold-table analysis. Only data obtained from animals with ROSC were analyzed. The data are expressed as mean ± SD. $P \leq 0.05$ was considered significant. $P > 0.05$ was defined as not significant (NS).

Results

Expression of p35 in Rat Brain

Levels of p35 transgene (fig. 1, *A*) mRNA expression were analyzed by Northern blotting (fig. 1, *B*).[40] The size of the bulk of transgene mRNA corresponded to polyadenylation occurring at the polyA site of the viral p35 gene. A small fraction of transgene mRNA species in brain and a significantly larger proportion of total transgene mRNA in thymus (fig. 1, *B*) were larger, as predicted from the desired splicing pattern of the chimeric transgene mRNA. In contrast to many other complementary DNA sequences that have been inserted and tested as transgenes in the Thy1 cassette (fig. 1, *A*), the viral p35 complementary DNA sequences seemed to cause some incompatibility with normal splicing in this cassette. Nevertheless, Western blot analysis using a rabbit polyclonal antibody to p35 revealed significant levels of p35 protein in both brain (fig. 1, *C* shows expression levels in a hippocampal extract) and thymus (data not shown). No aberrantly sized anti-p35 cross-reactive proteins were detected in transgenic rat tissue as compared with nontransgenic rat tissue. Therefore, it seems unlikely that the aberrantly sized transgene mRNAs gave rise to anomalous chimeric and/or p35 amino acid–containing proteins. Furthermore, we ruled out mutations introduced in the p35 gene while generating the rats. p35 coding sequences were retrieved from transgenic brain by reverse transcriptase polymerase chain reaction analysis and the correct sequence confirmed (data not shown). The highest levels of p35 transgene mRNA in brain were detected in the Thy1EμP35$_{L24}$ line, and the transgene mRNA distribution pattern was determined in the brain using *in situ* hybridization (figs. 1, *B* and *D*).

Table 2. Comparison of MAP during First Minutes of CPR Efforts, Duration of Resuscitation Procedures (CPR Time), and Number of Defibrillations between p35 Transgenic Animals and Their Nontransgenic Littermates (Wild-type)

	p35	Wild-type
MAP (mmHg) during CPR at		
0 min	0.3 ± 1.1	0.6 ± 1.5
1 min	38.6 ± 7.4	40.9 ± 7.2
2 min	38.8 ± 4.3	40.0 ± 7.8
3 min	34.4 ± 9.2	32.5 ± 12
CPR time (min)	2.8 ± 0.9	2.7 ± 0.8
Maximal MAP (mmHg) during CPR	42.1 ± 5.3	43.3 ± 7.4
Time until maximal MAP during CPR (min)	1.3 ± 0.4	1.4 ± 0.6
No. of defibrillations	2.3 ± 1.4	2.6 ± 1.4

Values are expressed as mean ± SD.

No statistical differences could be detected between the p35 transgenic rats and their nontransgenic littermates.

CPR = cardiopulmonary resuscitation; MAP = mean arterial pressure.

Cardiac Arrest and Cardiopulmonary Resuscitation

Before cardiac arrest, hemodynamic and physiologic variables were similar in the transgenic rats and nontransgenic rat littermates (table 1). Transesophageal electrical fibrillation led to circulatory arrest within 15 s in all experimental animals. No spontaneous defibrillations were observed during the period of circulatory arrest. Cardiopulmonary resuscitation (table 2) in terms of ROSC was successful in 92% of the transgenic animals (12 of 13) and in 68% of the nontransgenic animals (17 of 25; $P = 0.09$) (fig. 2). In successfully resuscitated animals, there were no significant differences between the two groups with regard to the duration of cardiopulmonary resuscitation (transgenic rats, 2.8 ± 0.9 min; controls, 2.7 ± 0.8 min; table 2), the number of direct current countershocks (transgenic rats, 2.3 ± 1.4; controls, 2.6 ± 1.4; table 2), or the maximum mean arterial pressure during cardiopulmonary resuscitation (transgenic

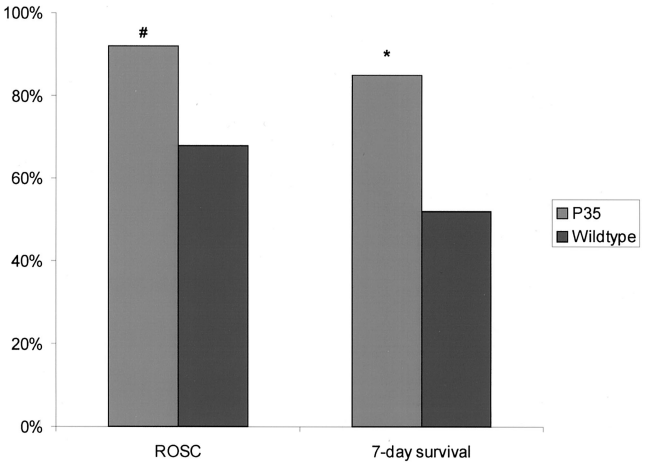

Fig. 2. Effects of p35 on restoration of spontaneous circulation (*ROSC*) and 7-day survival (# $P = 0.09$ *vs.* wild-type; * $P < 0.05$ *vs.* wild-type).

Table 3. Course of MAP during First 30 Min of ROSC in p35 Transgenic Rats and Their Nontransgenic Littermates (Wild-type)

	p35	Wild-type
MAP (mmHg)		
Immediately after ROSC	67.5 ± 32.1	75.9 ± 41.4
1 min after ROSC	81.3 ± 33.2	82.1 ± 36.4
2 min after ROSC	62.1 ± 30.9	65.3 ± 22.0
3 min after ROSC	53.1 ± 28.8	57.7 ± 20.0
4 min after ROSC	53.3 ± 19.7	61.2 ± 17.0
5 min after ROSC	66.1 ± 22.0	65.6 ± 18.9
10 min after ROSC	64.9 ± 19.7	66.1 ± 21.4
15 min after ROSC	68.5 ± 21.9	71.4 ± 17.5
20 min after ROSC	76.6 ± 16.8	82.0 ± 16.1
25 min after ROSC	71.4 ± 19.9	83.8 ± 12.6
30 min after ROSC	72.2 ± 10.1	81.7 ± 7.6
Maximal MAP after ROSC	100.0 ± 24.6	105.7 ± 34.7
Time of maximal MAP after ROSC (min)	8.0 ± 9.7	12.0 ± 20.8
Time to extubate (min)	18.5 ± 2.4	19.1 ± 2.6
Time to remove catheter (min)	30.5 ± 10.7	27.9 ± 3.6

Values are expressed as mean ± SD.

No statistical differences could be detected between the p35 transgenic rats and their nontransgenic littermates.

MAP = mean arterial pressure; ROSC = restoration of spontaneous circulation.

Table 4. Comparison of Results of Blood Gas Analyses at 5 and 20 Min after Restoration of Spontaneous Circulation

	p35	Wild-type
5 min after ROSC		
pH	7.2 ± 0.1	7.2 ± 0.1
P_{CO_2} (mmHg)	41.8 ± 12.2	44.3 ± 15.9
P_{O_2} (mmHg)	351.7 ± 89.8	331.6 ± 136.3
HCO_3 concentration (mM)	15.2 ± 3.9	16.0 ± 4.7
Base excess (mM)	−13.2 ± 4.4	−11.7 ± 4.8
Hemoglobin concentration (g/dL)	12.4 ± 1.4	12.1 ± 1.3
Hematocrit (%)	36.5 ± 3.9	36.0 ± 3.9
K^+ concentration (mM)	4.4 ± 1.0	4.1 ± 0.9
20 min after ROSC		
pH	7.0 ± 1.1	7.3 ± 0.1
P_{CO_2} (mmHg)	43.1 ± 6.2	42.3 ± 12.6
P_{O_2} (mmHg)	369.9 ± 138.1	320.9 ± 158.7
HCO_3 concentration (mM)	21.8 ± 4.4	19.9 ± 4.7
Base excess (mM)	−3.6 ± 6.5	−4.8 ± 7.2
Hemoglobin concentration (g/dL)	13.3 ± 1.2	13.6 ± 1.7
Hematocrit (%)	39.0 ± 3.2	39.3 ± 6.4
K^+ concentration (mM)	3.8 ± 0.6	4.0 ± 0.3

Values are expressed as mean ± SD.

No statistical differences could be detected between the p35 transgenic rats and their nontransgenic littermates.

ROSC = restoration of spontaneous circulation.

rats, 42.1 ± 5.3 mmHg; controls, 43.3 ± 7.4 mmHg; table 2).

Early Reperfusion after Cardiac Arrest

After return of spontaneous cardiac function, the blood pressure rose markedly in both transgenic and nontransgenic rats (table 3). In general, within the first 2 min, it peaked at 100.0 ± 24.6 mmHg in the transgenic rats and at 105.7 ± 34.7 mmHg in the control animals (P = NS). Then it returned to or below baseline, depending on the animal, but there were no major differences between transgenic and control groups. Cardiac arrest and cardiopulmonary resuscitation led to severe metabolic disturbances, as demonstrated by a decrease in arterial pH and base excess without significant differences between the investigated groups (table 4). Buffering with $NaHCO_3$ and regulating ventilation led to a return to almost normal values of the blood gas parameters within 20 min (with the exception of P_{O_2} as the consequence of ventilation with 100% O_2; table 4).

Overall Survival

Survival after cardiac arrest was monitored for 7 days, and the survival rate was 85% in the transgenic group (11 of 13) *versus* 52% in the control group (13 of 25; $P < 0.05$) (table 5; fig. 2). As mentioned above, resuscitation was achieved in 12 of 13 p35 transgenic animals and in 17 of 25 of their nontransgenic littermates, resulting in 8% unsuccessfully resuscitated p35 transgenic rats and 32% unsuccessfully resuscitated wild-type littermates. Once resuscitated, 1 (8%) of 12 transgenic animals died during the 7-day observation period in comparison with 4 (24%) of 17 nontransgenic littermates. Therefore, the probability of an unsuccessful resuscitation was approximately six times higher in wild-type animals than in the p35 transgenic rats (odds ratio = 5.6; $P = 0.09$; fourfold-table analysis). In addition, once resuscitated, the probability of dying during the 7-day observation period was about three times higher in the wild-type animals than in the p35 transgenic animals (odds ratio = 3.38; $P = 0.28$; fourfold-table analysis).

NDS

The NDS was determined at 1, 3, and 7 days of reperfusion in the 24 surviving animals and showed substantial improvement with ongoing reperfusion (table 5). All animals were awake and active after 24 h but exhibited various coordination and sensory deficits as well as moderate spastic paralysis of the hind limbs. There were no differences between transgenic and nontransgenic animals with regard to the neurologic status on day 1 (transgenic rats, 42 ± 10; controls, 33 ± 16; P = NS). Coordination deficits and spastic paralysis declined in animals at 3 days; in the p35 transgenic animals, the score was significantly improved ($P < 0.05$). The intergroup difference in the NDS decrease was not significant (transgenic rats, 17 ± 8; controls, 18 ± 17; P = NS). After 7 days, most animals showed only slightly retarded reactions to visual stimulation and pinching of the tail or hind leg but no aggravating neurologic deficits (transgenic rats, 9 ± 7; controls, 9 ± 10). Scores for both wild-type and transgenic animals were significantly im-

Table 5. Histologic and Neurologic Analyses of p35 Transgenic Rats in Comparison with Wild-type Animals

	Viable Neurons	TUNEL-Positive Neurons	NDS			Survival Rate (%)
			1 d	3 d	7 d	
p35	9 ± 6	73 ± 77	42 ± 10	17 ± 8*	9 ± 7*	85†
Wild-type	8 ± 6	80 ± 19	33 ± 16	18 ± 17	9 ± 10*	52

Values are expressed as mean ± SD.

Neuronal viability and TUNEL-positive neurons were not significantly different by intergroup comparison. Improved recovery in the NDS over time could be observed first in the p35 transgenic group of resuscitated animals (* $P < 0.05$ *vs.* day 1). The long-term survival of p35 transgenic rats was substantially improved († $P < 0.05$ *vs.* wild-type).

NDS = neurologic deficit score; TUNEL = terminal deoxynucleotidyltransferase–mediated d-uracil triphosphate–biotin nick end-labeling.

proved in comparison with the neurologic status after day 1 ($P < 0.05$). Improved neurologic recovery, which was defined as worst NDS − best NDS in an individual animal of more than 30 points, was observed in 55% of the transgenic animals and 15% of the nontransgenic animals ($P = 0.055$).

Histologic Evaluation

As compared with control animals with no cardiac arrest (fig. 3, *A*), histologic evaluation of the hippocampal CA-1 sector at 7 days revealed severe neuronal damage in the two other groups (figs. 3, *B* and *C*). In transgenic animals, Nissl staining detected 9 ± 5 viable cells in the CA-1 areas investigated in the left hemisphere and 11 ± 3 viable cells in the CA-1 areas investigated in the right hemisphere. The nontransgenic controls had 9 ± 6 and 8 ± 6 surviving neurons, respectively, in the investigated areas (P = NS *vs.* transgenic animals). Additional investigation revealed further neuronal degeneration in the hippocampal CA-3 sector, dentate gyrus, neocortex, and thalamus (data not shown; P = NS for transgenic *vs.* control animals).

Observations from TUNEL Staining

TUNEL staining (fig. 3) revealed DNA fragmentation in neurons of the hippocampal CA-1 sector of the two hemispheres in all animals investigated (figs. 3, *B* and *C*). In control animals without cardiac arrest, we did not detect any TUNEL-positive neurons (fig. 3, *D*). No differences in TUNEL staining were observed between the two groups. At 7 days after cardiac arrest, investigation of the hippocampal CA-1 sector in the nontransgenic controls revealed 80 ± 19 TUNEL-positive cells in the left hemisphere and 79 ± 15 TUNEL-positive cells in the right hemisphere (cells per area investigated; fig. 3, *E*; P = NS). In the transgenic group, we found 73 ± 7 TUNEL-positive neurons in the left hemisphere and 79 ± 13 TUNEL-positive neurons in the right hemisphere in the hippocampal CA-1 sector (cells per area investigated; fig. 3, *F*). Further analysis at higher magnifications revealed no detectable neurodegeneration in control animals (fig. 3, *G*); however, in both groups with cardiac arrest, about 30% of TUNEL-positive nuclei in the hippocampal CA-1 sector showed condensed chromatin and apoptotic bodies (figs. 3, *H* and *I*) after 7 days of reperfusion.

Discussion

The present study demonstrates for the first time the effects of transgenic expression of baculovirus p35 in

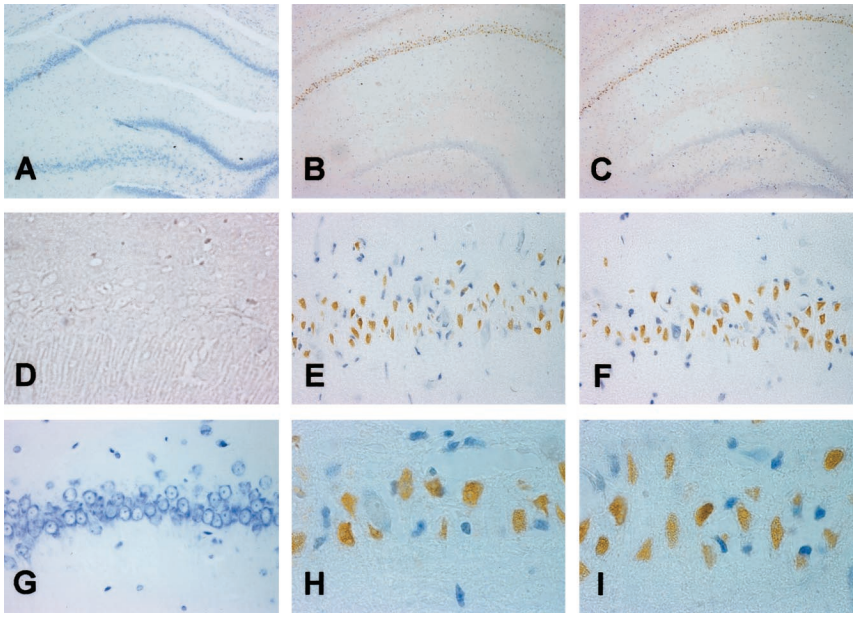

Fig. 3. Views of the hippocampus in sham-operated (*A*), wild-type (*B*), and p35 transgenic (*C*) animals at 7 days after 6 min of cardiac arrest. Terminal deoxynucleotidyltransferase–mediated d-uracil triphosphate–biotin nick end-labeling (TUNEL) staining (*D*) and histologic evaluation (*G*) revealed no detectable degeneration in sham-operated controls. Higher magnification of the hippocampal cornu ammonis 1 sector subfield shows severe neuronal damage in wild-type (*E*) and transgenic (*F*) animals at 7 days after 6 min of cardiac arrest. In both wild-type (*H*) and transgenic (*I*) animals, TUNEL-positive nuclei with apoptotic morphologic characteristics could be detected.

postnatal central neurons after global cerebral ischemia due to cardiocirculatory arrest in rats. The rate of ROSC, 7-day survival rate, quality of neurologic recovery, and amount of neuronal cell damage in the hippocampal CA-1 sector were determined. Detection of TUNEL-positive neurons with condensed chromatin in transgenic and nontransgenic rats suggests an apoptosis-associated pattern of neuronal degeneration after cardiac arrest. Interestingly, however, inhibition of caspase with p35 showed no positive effect on neuronal degeneration and neurologic outcome. Therefore, apoptosis in hippocampal neurons after cardiac arrest may not be primarily initiated by activation of caspases. A significant increase in 7-day survival, however, was observed in p35 transgenic animals, suggesting that antiapoptotic protein p35 plays an important role in postischemic recovery after cardiac arrest.

Cells undergoing apoptotic cell death reveal a characteristic sequence of cytologic alterations, including membrane blebbing and nuclear and cytoplasmic condensation. Moreover, apoptosis is characterized by specific internucleosomal DNA fragmentation, resulting in the typical "DNA laddering" in gel electrophoresis.[11,41,42] It cannot be excluded, however, that DNA fragmentation also occurs in cells not showing the typical morphologic characteristics of apoptosis.[43,44] TUNEL staining, therefore, may also label DNA fragments induced by other pathologic processes, including necrotic cell death. The random DNA fragmentation in nuclei damaged due to necrosis may, however, lead to more diffuse staining by the TUNEL technique.[11,42] In the present study, TUNEL staining revealed condensed chromatin and apoptotic bodies in about one third of the TUNEL-positive nuclei of hippocampal CA-1 neurons at 7 days. Apoptotic morphologic characteristics were observed in both p35 transgenic animals and nontransgenic littermates. Therefore, histologic evidence supports the view that at least some of the CA-1 neurons might undergo apoptosis after global cerebral ischemia due to cardiac arrest. These data are in line with previous results obtained from other models of global cerebral ischemia[11,42,45] and with data from our group, demonstrating that caspase 3, an effector of the cell death program, is activated at both the transcriptional and the posttranscriptional level in the rat hippocampal CA-1 sector after 10 min of cardiac arrest.[15] The construction of transgenic rats made it possible to explore the hypothesis of the beneficial properties of the broad-spectrum antiapoptotic baculovirus caspase inhibitor p35 *in vivo* in a model of global cerebral ischemia and reperfusion. In several *in vitro* studies, protective effects of p35 have been documented,[46] similar to those for synthetic inhibitors such as DEVD-FMK or VAD-FMK.[15,18]

In the present study, Thy1-driven expression of antiapoptotic p35 was found exclusively in the rat brain and to a lesser extent in the thymus. In all other tissues, no detectable levels of p35 could be demonstrated. Because of the late onset of neuronal expression with the Thy1 cassette, no disturbances in normal development were detected. Accordingly, the physiologic data did not reveal any differences between the transgenic rats and their nontransgenic littermates. p35 can inhibit the mammalian caspases 1, 3, 6, 7, 8, and 10, with inhibitory constant values of less than 10 nM, and form an inhibitory complex with these caspases after it is cleaved at its P1 residue (aspartic acid No.:87).[47] Despite this broad-spectrum inhibitory capacity, we did not observe any effect in inhibition of neuronal cell death in the CA-1 sector in the analysis either by TUNEL or by histologic examination. In addition, the NDSs after 1, 3, and 7 days did not demonstrate any differences between wild-type and transgenic animals. Therefore, the present data suggest that at least the pathway that is influenced by p35 (caspases) is not primarily relevant for neuronal degeneration and delayed neuronal death in the hippocampal CA-1 sector after global ischemia due to cardiac arrest in rats. It is, therefore, possible that another cascade of apoptotic events is activated after global cerebral ischemia, *e.g.*, activation of noncaspase proteases,[48] resulting in an ineffectiveness of p35 expression. In this regard, a substantial amount of evidence has recently been reported, which outlines the important role of caspase-independent programmed cell death with or without apoptotic morphologic characteristics[49–51] (*e.g.*, activation of calpain or the lysosomal cathepsins[52]).

Most interestingly, the 7-day survival rate was significantly better in the p35 transgenic group. In addition, we observed a higher initial rate of ROSC ($P = 0.09$) in p35 transgenic animals than in nontransgenic animals. The neurologic recovery after cardiac arrest in p35 transgenic animals was enhanced ($P = 0.055$) as compared with nontransgenic controls. These findings cannot be explained by the morphologic data in the CA-1 sector, showing no difference in neuronal survival between groups. Explanations for the underlying mechanisms of improved survival are still speculative. It is entirely possible that the process of creating the transgenic animals altered something other than caspase activity or that p35 has other effects, but we have no evidence in support of these assumptions. Whatever the function of p35 here, we assume that it is not related to the brain, because it did not influence neurologic function or histopathologic evidence of apoptosis in the surviving animals. Concerning the p35 expression in thymus-derived cells, microcirculatory reperfusion might be influenced by blood viscosity, coagulation, or inflammation. Most recently, marked activation of complement and polymorphonuclear leukocytes and increased polymorphonuclear leukocyte–endothelial interaction during cardiopulmonary resuscitation and early reperfusion after cardiac arrest in humans were demonstrated.[53] Therefore, similar effects

could not be excluded as the cause of the observed effect of enhanced survival in the transgenic animals.

Overall, limitations of our study were the unavailability of a "dose–response curve," which could only be circumvented by the use of different strains of p35 transgenic animals, and the appropriate measurement of caspase 3 activity. In the latter case, we were not able to perform an activity assay of caspase 3 due to the perfusion fixation protocol that was used.

In conclusion, detection of TUNEL-positive neurons with condensed chromatin in the hippocampal CA-1 sector after 6 min of global cerebral ischemia due to cardiocirculatory arrest suggests an apoptosis-associated pattern of neuronal degeneration. Inhibition of caspases with the broad-spectrum inhibitor p35, however, showed no positive effect on neuronal degeneration and neurologic outcome after cardiac arrest in rats. Therefore, the present data suggest that neuronal apoptosis after cardiac arrest is probably not initiated by activation of caspases. Most interestingly, however, a marked increase in the 7-day survival was observed in p35 transgenic animals, even if only successfully resuscitated animals were considered, suggesting that the antiapoptotic protein p35 plays an important role in postischemic recovery after cardiac arrest.

The authors thank Harry Bauer, M.D. (Research Fellow at the Department of Anesthesiology, University of Heidelberg, Heidelberg, Germany), for excellent statistical advice.

References

1. Brain Resuscitation Clinical Trial II Study Group: A randomized clinical study of a calcium-entry blocker (lidoflazine) in the treatment of comatose survivors of cardiac arrest. N Engl J Med 1991; 324:1225–31
2. Brain Resuscitation Clinical Trial I Study Group: Randomized clinical study of thiopental loading in comatose survivors of cardiac arrest. N Engl J Med 1986; 314:397–403
3. The Hypothermia after Cardiac Arrest Study Group: Mild therapeutic hypothermia to improve the neurologic outcome after cardiac arrest. N Engl J Med 2002; 346:549–56
4. Bernard SA, Gray TW, Buist MD, Jones BM, Silvester W, Gutteridge G, Smith K: Treatment of comatose survivors of out-of-hospital cardiac arrest with induced hypothermia. N Engl J Med 2002; 346:557–63
5. Padosch SA, Kern KB, Böttiger BW: Therapeutic hypothermia after cardiac arrest. N Engl J Med 2002; 347:63–5
6. Böttiger BW, Bode C, Kern S, Gries A, Gust R, Glatzer R, Bauer H, Motsch J, Martin E: Efficacy and safety of thrombolytic therapy after initially unsuccessful cardiopulmonary resuscitation: A prospective clinical trial. Lancet 2001; 357: 1583–5
7. Böttiger BW, Padosch SA, Wenzel V: Tissue plasminogen activator in cardiac arrest with pulseless electrical activity. N Engl J Med 2002; 347:1281–2
8. Hossmann K-A: Disturbances of cerebral protein synthesis and ischemic cell death. Prog Brain Res 1993; 96:161–77
9. Safar P: Cerebral resuscitation after cardiac arrest: A review. Circulation 1986; 74(suppl IV):IV138–53
10. Böttiger BW, Schmitz B, Wiessner C, Vogel P, Hossmann KA: Neuronal stress response and neuronal cell damage after cardiocirculatory arrest in rats. J Cereb Blood Flow Metab 1998; 18:1077–87
11. Choi DW: Ischemia-induced neuronal apoptosis. Curr Opin Neurobiol 1996; 6:667–72
12. Thornberry NA: Caspases: Key mediators of apoptosis. Chem Biol 1998; 5:R97–103
13. Villa P, Kaufmann SH, Earnshaw WC: Caspases and caspase inhibitors. Trends Biochem Sci 1997; 22:388–93
14. Cohen GM: Caspases: The executioners of apoptosis. Biochem J 1997; 326:1–16
15. Gillardon F, Böttiger BW, Schmitz B, Zimmermann M, Hossmann K-A: Activation of CPP-32 protease in hippocampal neurons following ischemia and epilepsy. Mol Brain Res 1997; 50:16–22
16. Hara H, Friedlander RM, Gagliardini V, Ayata C, Fink K, Huang Z, Shimizu-Sasamata M, Yuan J, Moskowitz MA: Inhibition of interleukin 1beta converting enzyme family proteases reduces ischemic and excitotoxic neuronal damage. Proc Natl Acad Sci U S A 1997; 94:2007–12
17. Endres M, Namura S, Shimizu-Sasamata M, Waeber C, Zhang L, Gomez-Isla T, Hyman BT, Moskowitz MA: Attenuation of delayed neuronal death after mild focal ischemia in mice by inhibition of the caspase family. J Cereb Blood Flow Metab 1998; 18:238–47
18. Wiessner C, Sauer D, Alaimo D, Allegrini PR: Protective effect of a caspase inhibitor in models for cerebral ischemia in vitro and in vivo. Cell Mol Biol (Noisy-le-grand) 2000; 46:53–62
19. Friedlander RM, Gagliardini V, Hara H, Fink KB, Li W, MacDonald G, Fishman MC, Greenberg AH, Moskowitz MA, Yuan J: Expression of a dominant negative mutant of interleukin-1 beta converting enzyme in transgenic mice prevents neuronal cell death induced by trophic factor withdrawal and ischemic brain injury. J Exp Med 1997; 185:933–40
20. Schielke GP, Yang GY, Shivers BD, Betz AL: Reduced ischemic brain injury in interleukin-1 beta converting enzyme-deficient mice. J Cereb Blood Flow Metab 1998; 18:180–5
21. Wang S, Miura M, Jung YK, Zhu H, Li E, Yuan J: Murine caspase-11, an ICE-interacting protease, is essential for the activation of ICE. Cell 1998; 92:501–9
22. Shibata M, Hisahara S, Hara H, Yamawaki T, Fukuuchi Y, Yuan J, Okano H, Miura M: Caspases determine the vulnerability of oligodendrocytes in the ischemic brain. J Clin Invest 2000; 106:643–53
23. Holtzman DM, Deshmukh M: Caspases: A treatment target for neurodegenerative disease? Nat Med 1997; 3:954–5
24. Zhou Q, Krebs JF, Snipas SJ, Price A, Alnemri ES, Tomaselli KJ, Salvesen GS: Interaction of the baculovirus anti-apoptotic protein p35 with caspases: Specificity, kinetics, and characterization of the caspase/p35 complex. Biochemistry 1998; 37:10757–65
25. Pettmann B, Henderson CE: Neuronal cell death. Neuron 1998; 20:633–47
26. Xue D, Horvitz HR: Inhibition of the Caenorhabditis elegans cell-death protease CED-3 by a CED-3 cleavage site in baculovirus p35 protein. Nature 1995; 377:248–51
27. Bump NJ, Hackett M, Hugunin M, Seshagiri S, Brady K, Chen P, Ferenz C, Franklin S, Ghayur T, Li P, Licari P, Mankovich J, Shi L, Greenber AH, Miller LK, Wong WW: Inhibition of ICE family proteases by baculovirus antiapoptotic protein p35. Science 1995; 269:1885–8
28. Robertson NM, Zangrilli J, Fernandes-Alnemri T, Friesen PD, Litwack G, Alnemri ES: Baculovirus P35 inhibits the glucocorticoid-mediated pathway of cell death. Cancer Res 1997; 57:43–7
29. White K, Tahaoglu E, Steller H: Cell killing by the Drosophila gene reaper. Science 1996; 271:805–7
30. Bose R, Chen P, Loconti A, Grullich C, Abrams JM, Kolesnick RN: Ceramide generation by the Reaper protein is not blocked by the caspase inhibitor, p35. J Biol Chem 1998; 273:28852–9
31. Martinou I, Fernandez PA, Missotten M, White E, Allet B, Sadoul R, Martinou JC: Viral proteins E1B19K and p35 protect sympathetic neurons from cell death induced by NGF deprivation. J Cell Biol 1995; 128:201–8
32. Texido G, Eibel H, Le Gros G, van der Putten H: Transgene CD23 expression on lymphoid cells modulates IgE and IgG1 responses. J Immunol 1994; 153:3028–42
33. Moll J, Schmidt A, van der Putten H, Plug R, Ponta H, Herrlich P, Zoller M: Accelerated immune response in transgenic mice expressing rat CD44v4-v7 on T cells. J Immunol 1996; 156:2085–94
34. Wiessner C, Allegrini PR, Rupalla K, Sauer D, Oltersdorf T, McGregor AL, Bischoff S, Böttiger BW, van der Putten H: Neuron-specific transgene expression of Bcl-XL but not Bcl-2 genes reduced lesion size after permanent middle cerebral artery occlusion in mice. Neurosci Lett 1999; 268:119–22
35. Böttiger BW, Krumnikl JJ, Gass P, Schmitz B, Motsch J, Martin E: The cerebral "no-reflow" phenomenon after cardiac arrest in rats: Influence of low-flow reperfusion. Resuscitation 1997; 34:79–87
36. Katz L, Ebmeyer U, Safar P, Radovsky A, Neumar R: Outcome model of asphyxial cardiac arrest in rats. J Cereb Blood Flow Metab 1995; 15:1032–9
37. Neumar RW, Bircher NG, Sim KM, Xiao F, Zadach KS, Radovsky A, Katz L, Ebmeyer E, Safar P: Epinephrine and sodium bicarbonate during CPR following asphyxial cardiac arrest in rats. Resuscitation 1995; 29:249–63
38. Gavrieli Y, Sherman Y, Ben-Sasson SA: Identification of programmed cell death in situ via specific labeling of nuclear DNA fragmentation. J Cell Biol 1992; 119:493–501
39. Wiessner C, Brink I, Lorenz P, Neumann-Haefelin T, Vogel P, Yamashita K: Cyclin D1 messenger RNA is induced in microglia rather than neurons following transient forebrain ischemia. Neuroscience 1996; 72:947–58
40. Luthi A, Putten H, Botteri FM, Mansuy IM, Meins M, Frey U, Sansig G, Portet C, Schmutz M, Schroder M, Nitsch C, Laurent JP, Monard D: Endogenous serine protease inhibitor modulates epileptic activity and hippocampal long-term potentiation. J Neurosci 1997; 17:4688–99
41. Appleby DW, Modak SP: DNA degradation in terminally differentiating lens fiber cells from chick embryos. Proc Natl Acad Sci U S A 1977; 74:5579–83
42. Charriaut-Marlangue C, Margaill I, Represa A, Popovici T, Plotkine M,

Ben-Ari Y: Apoptosis and necrosis after reversible focal ischemia: An in situ DNA fragmentation analysis. J Cereb Blood Flow Metab 1996; 16:186–94

43. Chopp M, Li Y, Jiang N, Zhang RL, Prostak J: Antibodies against adhesion molecules reduce apoptosis after transient middle cerebral artery occlusion in rat brain. J Cereb Blood Flow Metab 1996; 16:578–84

44. Li Y, Chopp M, Jiang N, Yao F, Zaloga C: Temporal profile of in situ DNA fragmentation after transient middle cerebral artery occlusion in the rat. J Cereb Blood Flow Metab 1995; 15:389–97

45. Heron A, Pollard H, Dessi F, Moreau J, Lasbennes F, Ben Ari Y, Charriaut Marlangue C: Regional variability in DNA fragmentation after global ischemia evidenced by combined histological and gel electrophoresis observations in the rat brain. J Neurochem 1993; 61:1973–6

46. Viswanath V, Wu Z, Fonck C, Wei Q, Boonplueang R, Andersen JK: Transgenic mice neuronally expressing baculoviral p35 are resistant to diverse types of induced apoptosis, including seizure-associated neurodegeneration. Proc Natl Acad Sci U S A 2000; 97:2270–5

47. Ekert PG, Silke J, Vaux DL: Caspase inhibitors. Cell Death Differ 1999; 6:1081–6

48. Borner C, Monney L: Apoptosis without caspases: An inefficient molecular guillotine? Cell Death Differ 1999; 6:497–507

49. Johnson DE: Noncaspase proteases in apoptosis. Leukemia 2000; 14:1695–703

50. Leist M, Jaattela M: Four deaths and a funeral: From caspases to alternative mechanisms. Nat Rev Mol Cell Biol 2001; 2:589–98

51. Mathiasen IS, Jaattela M: Triggering caspase-independent cell death to combat cancer. Trends Mol Med 2002; 8:212–20

52. Yamashima T: Implication of cysteine proteases calpain, cathepsin and caspase in ischemic neuronal death of primates. Prog Neurobiol 2000; 62:273–95

53. Böttiger BW, Motsch J, Braun V, Martin E, Kirschfink M: Marked activation of complement and leukocytes and an increase in the concentrations of soluble endothelial adhesion molecules during cardiopulmonary resuscitation and early reperfusion after cardiac arrest in humans. Crit Care Med 2002; 30:2473–80